ARTICLE

ACS chemical biology

Nontoxic Chemical Interdiction of the Epithelial-to-Mesenchymal Transition by Targeting Cap-Dependent Translation

Brahma Ghosh[†,§], Alexey O. Benyumov[‡,§], Phalguni Ghosh[†], Yan Jia[†], Svetlana Avdulov[‡], Peter S. Dahlberg[‡], Mark Peterson[‡], Karen Smith[‡], Vitaly A. Polunovsky[‡], Peter B. Bitterman[‡], and Carston R. Wagner[†,*]

Departments of [†]Medicinal Chemistry and [‡]Medicine, University of Minnesota, Minneapolis, Minnesota 55455. [§]These authors contributed equally to this work.

ABSTRACT Normal growth and development depends upon high fidelity regulation of cap-dependent translation initiation, a process that is usurped and redirected in cancer to mediate acquisition of malignant properties. The epithelial-to-mesenchymal transition (EMT) is a key translationally regulated step in the development of epithelial cancers and pathological tissue fibrosis. To date, no compounds targeting EMT have been developed. Here we report the synthesis of a novel class of histidine triad nucleotide binding protein (HINT)-dependent pronucleotides that interdict EMT by negatively regulating the association of eIF4E with the mRNA cap. Compound eIF4E inhibitor-1 potently inhibited cap-dependent translation in a dose-dependent manner in zebrafish embryos without causing developmental abnormalities and prevented eIF4E from triggering EMT in zebrafish ectoderm explants without toxicity. Metabolism studies with whole cell lysates demonstrated that the prodrug was rapidly converted into 7-BnGMP. Thus we have successfully developed the first nontoxic small molecule able to inhibit EMT, a key process in the development of epithelial cancer and tissue fibrosis, by targeting the interaction of eIF4E with the mRNA cap and demonstrated the tractability of zebrafish as a model organism for studying agents that modulate EMT. Our work provides strong motivation for the continued development of compounds designed to normalize cap-dependent translation as novel chemo-preventive agents and therapeutics for cancer and fibrosis.

Recruitment of the small ribosome subunit to the 5′ end of mRNA is the rate-controlling step in the initiation of eukaryotic protein synthesis. For the majority of eukaryotic transcripts, this process requires assembly of the heterotrimeric translation initiation complex eIF4F and its association with the 7-MeGTP (m7GpppX) cap structure at the 5′ end of mRNA (*1–4*). The eIF4F complex consists of eIF4E, the mRNA cap-binding protein; eIF4A, a helicase; and eIF4G, a docking protein that associates with the 40S ribosomal subunit *via* contact with the multimeric adapter complex eIF3 (*5*). Under physiological conditions, eIF4E is the least abundant component of the initiation machinery and therefore controls the rate of translation initiation (*6*).

The translation initiation apparatus functions as a key regulatory hub in the flow of genetic information from the genome to the proteome (*7–9*). Normal growth and development features high fidelity regulation of transcript egress from the nucleus and ribosome recruitment (*10, 11*). In contrast, cancer is characterized by unrestrained activation of the translation initiation machinery, altering the genome-wide pattern of translation initiation to favor cell autonomous function (*12–15*). This has generated considerable interest in the translation initiation machinery as a target for rational anticancer therapy (*7, 16*).

The eIF4E–eIF4G binding step has been successfully targeted in cancer models (*17*); however, this approach may be limited by its lack of selectivity for cancer-related translation initiation. Targeting the interaction of eIF4E with the cap may afford a means to overcome this limi-

*Corresponding author, wagne003@umn.edu.

Received for review August 8, 2008 and accepted April 6, 2009.

Published online April 7, 2009

10.1021/cb9000475 CCC: $40.75

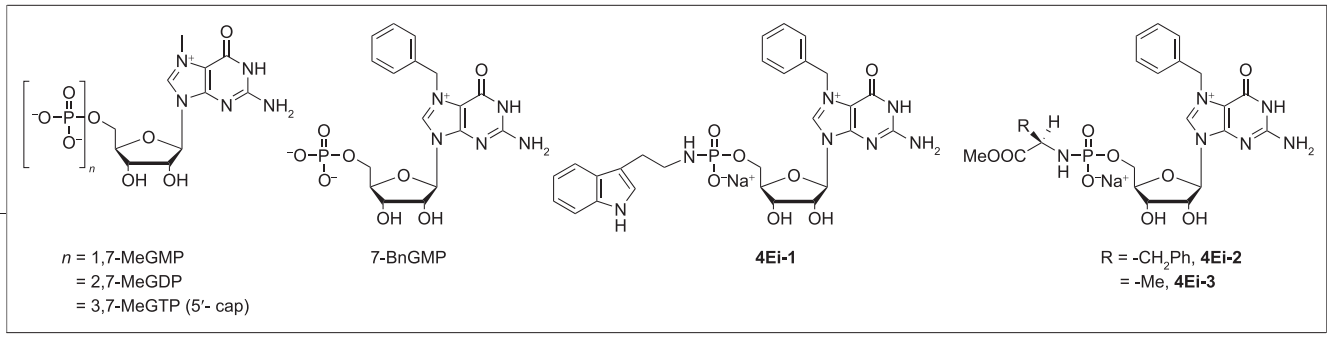

Figure 1. Chemical structure of cap analogues.

tation. The efficiency of two key eIF4E-dependent steps in translation initiation, transcript egress from the nucleus and ribosome recruitment, varies widely among transcripts, with those encoding potentially oncogenic proteins showing a disproportionate dependence on the association of eIF4E with its cap. We propose to exploit this natural selectivity. One approach that has shown promise is indirect: using an RNA interference strategy to decrease the abundance of eIF4E (*16, 18*). An alternative approach that we have taken is direct: using synthetic nucleotide derivatives such as 7-benzyl guanosine monophosphate (7-BnGMP) to block the binding of eIF4E to the mRNA cap (*19, 20*). Unfortunately, while effective in cell-free systems, its efficacy in cells is low. One approach to improving *in vivo* activity is to develop a stable pro-drug (pronucleotide) that can be converted into an active species by the target cell (*21, 22*). Phosphoramidates are a promising class of compounds for this purpose. They are water-soluble, nontoxic, and stable and have been used in humans as potent antiviral and antitumor agents (*23–27*). They display significantly longer *in vivo* half-lives and greater volumes of distribution compared to those of their parent nucleotides (*26, 27*). Nucleoside phosphoramidates can be converted efficiently inside the cell into their corresponding 5′-monophosphate nucleotide by a family of phosphoramidase enzymes called histidine triad nucleotide binding proteins (HINT) (*28–30*). Human HINT-1 (hHINT-1) binds preferentially to purine analogues (*29*) and is aberrantly expressed in cancer cells (*31*). The enzyme prefers phosphoramidates with unhindered primary amines and tolerates substitutions at the N-7 position of the purine base without loss of substrate specificity (*29*).

As a first step toward our goal, we report the successful implementation of a pronucleotide strategy for the intracellular release of 7-BnGMP to inhibit cap-dependent translation. By introducing a suitable alkyl or aryl-alkyl substituent at the N-7 position, we achieved dose-dependent inhibition of cap-dependent translation in zebrafish eggs/embryos without disturbing development and, using zebrafish ectoderm explants, effectively blocked the epithelial-to-mesenchymal transition (EMT), a key step in the genesis of epithelial cancers and tissue fibrosis, with no apparent toxicity (*32–36, 37, 38*).

RESULTS AND DISCUSSION

Affinity of Cap Analogues for eIF4E. We synthesized a 12-member library of 7-alkylated 5′-aryl amine/amino acid phosphoramidates of guanosine and quantified affinity for three representative examples (Figure 1) by fluorescence quenching. Removal of the γ- and β-units of the phosphate chain led to a significant fall in K_d (Table 1) in accord with the published literature (*39*). This underscores the role played by the phosphate backbone in the recognition of the 5′-cap by the lysine and arginine residues of the eIF4E cap-binding site (*40*).

The strength of the interaction between eIF4E and the nucleotide monophosphates increased when the methyl substituent at N7 was replaced by a benzyl group. Thus, 7-BnGMP showed a 10-fold increase in binding affinity compared to 7-MeGMP (Table 1). Crystal structure determination and analysis of eIF4E complexed with 7-BnGMP and a 4E-BP1 peptide revealed that conformational changes in the cap-binding site induced by the presence of the benzyl substituent allows it to pack into a hydrophobic cavity dorsal to the π-stacked tryptophans (W56 and W102) of the eIF4E active site (*41*). This added interaction partly compensates for the decreased binding affinity incurred with the loss of two phosphate units.

TABLE 1. Comparison of dissociation constants (K_d) for the phosphoramidates and cap analogues by fluorescence quenching

Compounds	K_d (μM)	$K_d/K_{d7\text{-MeGTP}}$
7-MeGTP	0.010 ± 0.003	1
7-MeGMP	7.5 ± 0.4	750
7-BnGMP	0.800 ± 0.060	80
4Ei-1	31.0 ± 1.0	3100
4Ei-2	81.0 ± 12.8	8100
4Ei-3	55.02 ± 7.4	5500

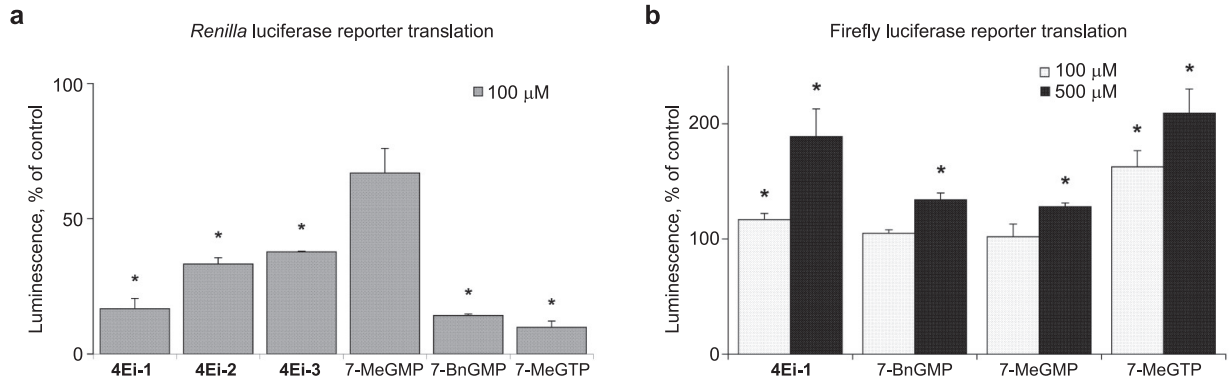

Figure 2. Inhibition of cap-dependent translation by cap analogues *in vitro*. a) Cap-dependent translation quantified as the expression of *Renilla* luciferase reporter. b) IRES-mediated translation quantified as the expression of firefly luciferase reporter. Shown is the impact of compounds (100 and 500 μM) on reporter luminescence (arbitrary units) with all values normalized to the luminescence of a compound-free control reaction. Data are presented as mean ± SEM for 3 independent experiments; * indicates a significant difference at $p < 0.01$ compared to the calibration control set at 100.

The K_d for the cap-derived phosphoramidates (designated eIF4E-inhibitors, **"4Ei"**) followed the order **4Ei-1** < **4Ei-3** < **4Ei-2**. Our *in silico* simulation studies of **4Ei-1** complexed with eIF4E revealed that the indole side chain of the phosphoramidate resides within a concave hydrophobic pocket in the eIF4E active site (not shown). This may account for its greater affinity for the protein compared to the D-phenylalanine (**4Ei-2**) and D-alanine phosphoramidates (**4Ei-3**). The K_d value obtained for **4Ei-1** was, however, still 3200-fold higher than that for the natural substrate 7-MeGTP, indicating remarkably poor binding between **4Ei-1** and eIF4E.

Inhibition of Cap-Dependent Translation by Cap Analogues *in Vitro*. To directly evaluate how well our cap analogues inhibited cap-dependent translation, we employed a cell-free translation assay that uses the dual-luciferase mRNA, RLUC-POLIRES-FLUC, as a reporter. In this system, translation of *Renilla reniformis* luciferase (RLUC) is strictly cap-dependent, whereas translation of firefly luciferase (FLUC) proceeds in a cap-independent manner *via* an IRES (*42*). In accord with prior reports for a different class of small molecule inhibitors of cap-dependent translation (*17*), all active compounds stimulated IRES-mediated translation concomitantly with inhibition of cap-dependent translation at concentrations ≥100 μM (Figure 2). While most of the phosphoramidated 7-BnGMP derivatives revealed only marginal inhibitory potency compared to that of their parent compounds 7-BnGMP and 7-MeGTP, phosphoramidating 7-BnGMP with D-phenylalanine (**4Ei-2**) or D-alanine (**4Ei-3**) resulted in retention of more than 60% of the inhibitory activity, and tryptamine-phosphoramidated 7-BnGMP (**4Ei-1**) retained more than 80% of the inhibitory activity of the parent compounds, with an IC_{50} comparable to that of 7-BnGMP (16.7 ± 3.2 *vs* 15.9 ± 2.0 μM) (Table 2).

Since **4Ei-1** has been shown to be a substrate for human Hint1 and rabbit tissues have been previously shown to express the highly homologous (95%) rabbit Hint1, we examined the rabbit reticulocyte lysates for HINT1 activity. On the basis of endogenous phosphoramidase activity, the lysates were shown to possess 23 ng of active Hint per 20 μL of lysate. Thus, while **4Ei-1** has a low affinity for eIF4E, its ability to serve as a sub-

TABLE 2. Comparison of IC_{50} values determined for our lead compounds 4Ei-1 and 7-BnGMP to those of authentic cap analogues 7-MeGTP and 7-MeGMP

Suppression of cap-dependent translation	
Compounds	**IC_{50} (μM)**
4Ei-1	16.7 ± 3.2
7-BnGMP	15.9 ± 2.0
7-MeGTP	5.0 ± 0.6
7-MeGMP	200 ± 30

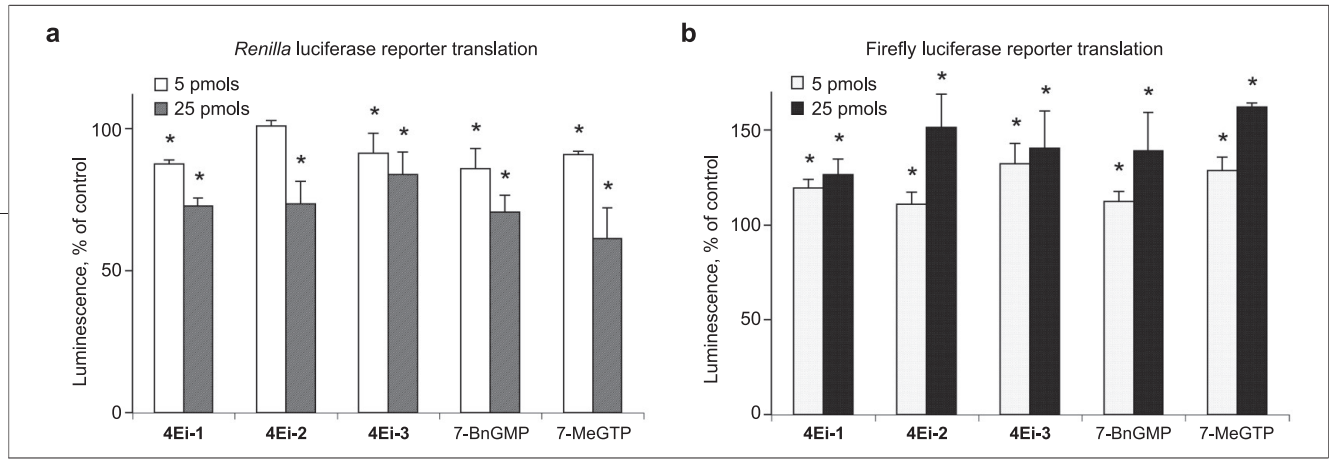

Figure 3. Inhibition of cap-dependent translation by cap analogues *in vivo*. a) Cap-dependent translation quantified as the expression of *Renilla* luciferase reporter. b) IRES-mediated translation quantified as the expression of firefly luciferase reporter. Shown is reporter translation for test compounds microinjected in doses of 5 and 25 pmols with all values normalized to the luminescence in embryos injected with HBSS. Data are presented as mean ± SEM for 3–5 independent experiments conducted with 20 embryos each; * indicates a significant difference at $p < 0.01$ compared to the HBSS calibration control set at 100.

strate for endogenous rabbit Hint1 enables it to be rapidly converted to the active species, 7-BnGMP.

One criterion for therapeutic potential is compound stability in a biological milieu. To assess this property, we preincubated compounds at 10–20 μM in the rabbit reticulocyte extract for 30 or 60 min. As evidenced by *Renilla* luciferase reporter activity, 7-MeGTP totally lost inhibitory activity within the first 30 min, whereas 7-BnGMP retained its level of activity for up to 60 min of preincubation (Supplementary Figure 1).

Inhibition of Cap-Dependent Translation by Cap Analogues *in Vivo*. The teleost zebrafish (*Danio rerio*) is a promising model organism for drug discovery that enables the testing of efficacy, toxicity, and biological activity in the same living system (*43, 44*). In order to examine compound efficacy and toxicity, we microinjected the dual-luciferase reporter mRNA and a test compound into freshly fertilized zebrafish eggs. For calibration, we co-injected eggs with the poison cycloheximide (CHD), which inhibits both cap-dependent and IRES-mediated reporter translation (Supplementary Figure 2). Consistent with our cell-free experiments, injections of **4Ei-1**, **-2**, or **-3** in doses ranging from 5 to 25 pmol per egg inhibited up to 30% of cap-dependent translation (Figure 3) without adverse effects on cell division or development (monitored for 96 h until completion of embryo development; data not shown). As seen in the cell-free system, introducing active compounds led to a dose-dependent increase in IRES-reporter translation, thereby excluding a nonspecific toxic effect of the compounds on the translational machinery or the organism itself. These findings indicate that 7-BnGMP and its phosphoramidated derivatives can inhibit cap-dependent translation by up to 30% in the physiological context of living vertebrate cells without cytotoxicity.

4Ei-1 Inhibits a Key Step in the Pathway to Cancer and Tissue Fibrosis, the Epithelial-to-Mesenchymal Transition. This result immediately raises the question of whether this level of translational inhibition is relevant to human disease. We sought to develop not only a novel system that featured a step in the genesis of cancer and tissue fibrosis that could be nullified but one that would also allow us to distinguish a specific biological effect from the nonspecific toxicity of inhibiting protein synthesis. For this purpose we chose a differentiation-dependent process in the cancer and fibrosis pathways, the epithelial-to-mesenchymal transition (EMT) (*45*). We generated a zebrafish explant model of EMT that is triggered by ectopic expression of eIF4E, an approach based on prior studies in *Xenopus laevis* (*46*). To validate the system, fertilized zebrafish eggs were co-injected with the dual luciferase reporter and mRNA encoding wild-type murine eIF4E carrying a hemaglutinin tag, "HA", noting that zebrafish and murine eIF4E-1A isoforms share 83% identity (Supplementary Figure 3). A cap-binding mutant (eIF4E W56A) served as a negative control, and *Xenopus* translation elongation factor-1α (xEF-1α) served as a neutral control. Expression and translational activity of exogenous wild-type eIF4E was readily detected in cell lysates 5 h post injection (Figure 4).

In our system, ectopic expression of eIF4E triggered EMT (Figure 5). After 24 h, explants from the embryos injected with eIF4E changed their shape from spherical to elliptical and began expressing the mesoderm-specific markers *no tail* (*ntl*) and *myogenic differentiation* (*myoD*). After 48 h, motile cells emerged. When explants were excised from embryos co-injected with 4E WT mRNA and **4Ei-1** (16 pmol), EMT was completely abrogated with no pathological changes in explant morphology, indicating the absence of toxicity (experimental details provided in Supplementary Table 1 and

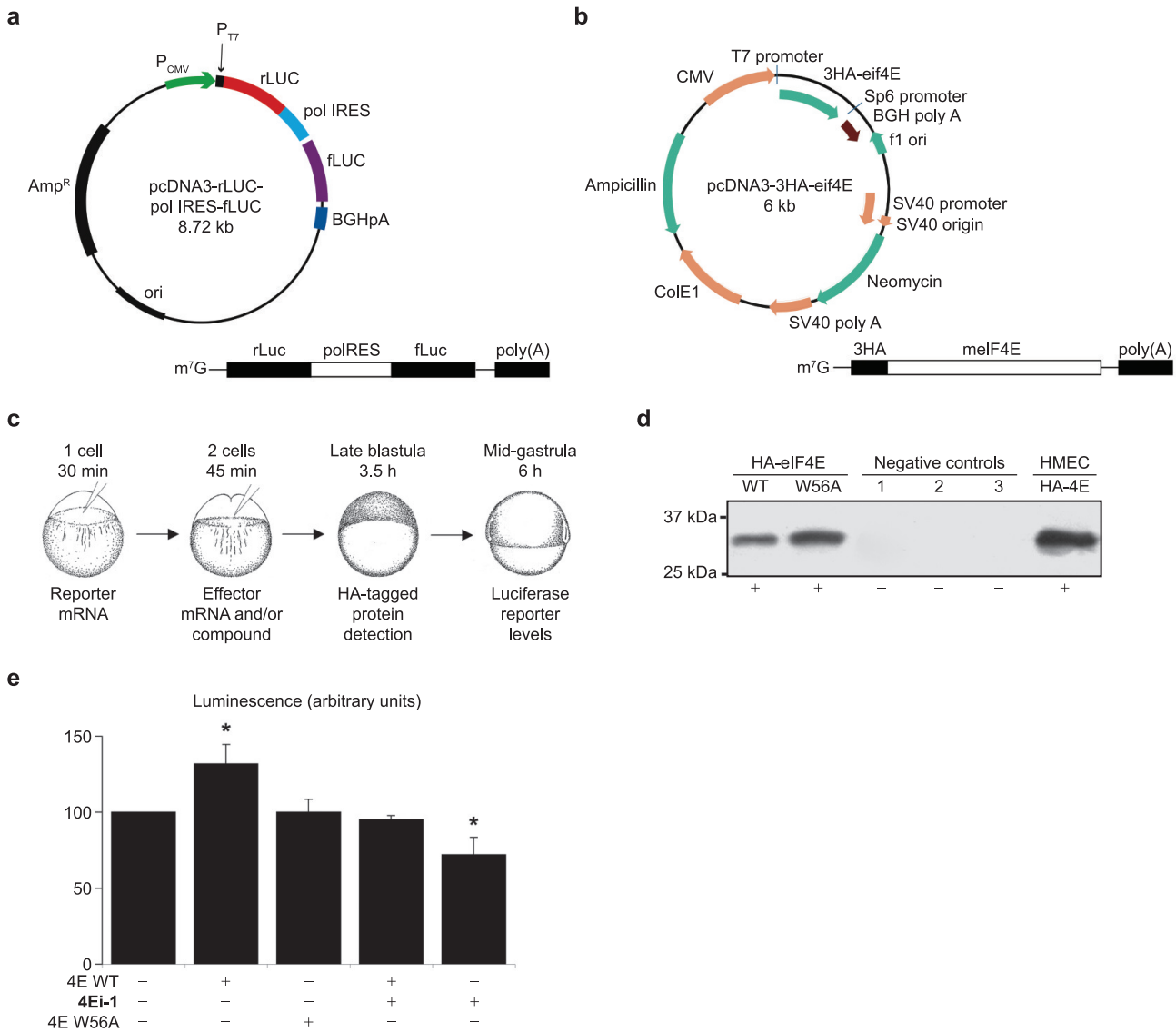

Figure 4. Manipulating cap-dependent translation in zebrafish embryos. a) Luciferase reporter mRNA transcribed *in vitro* from the construct pcDNA3-rLuc-polIRES-fLuc. b) mRNA encoding murine eIF4E WT or the cap binding mutant eIF4E W56A from the constructs pcDNA3-3HA-eIF4E-wt or -W56A. c) Experimental approach to analyze cap-dependent translation following genetic or pharmacological intervention. Luciferase reporter mRNA is microinjected at the one-cell stage. Effectors: (i) mRNA encoding the protein of interest (wt or mutant), (ii) translation inhibitor 4Ei-1, or (iii) both HA-eIF4E WT and 4Ei-1 are microinjected at the 2-cell stage. Half of the embryos are analyzed for expression of the HA-tagged exogenous proteins at the late blastula stage; the remaining embryos are analyzed at mid-gastrula for luminescence. d) Representative immunoblot demonstrating expression of exogenous wild-type and mutant eIF4E proteins in the injected embryos. Negative controls: lysates from xEF-1α- (1), buffer-injected (2) and noninjected embryos (3); Positive control: lysates from human mammary epithelial cells ectopically overexpressing eIF4E (HMEC/HA-4E). e) Impact of each treatment on *Renilla* luciferase reporter expression as a measure of cap-dependent translation, with all values normalized to the luminescence of embryos injected with xEF-1α (left bar). Data are presented as mean ± SEM for 3 independent experiments conducted with 20 embryos each; * indicates a significant difference at $p < 0.01$ compared to the xEF-1α calibration control set at 100.

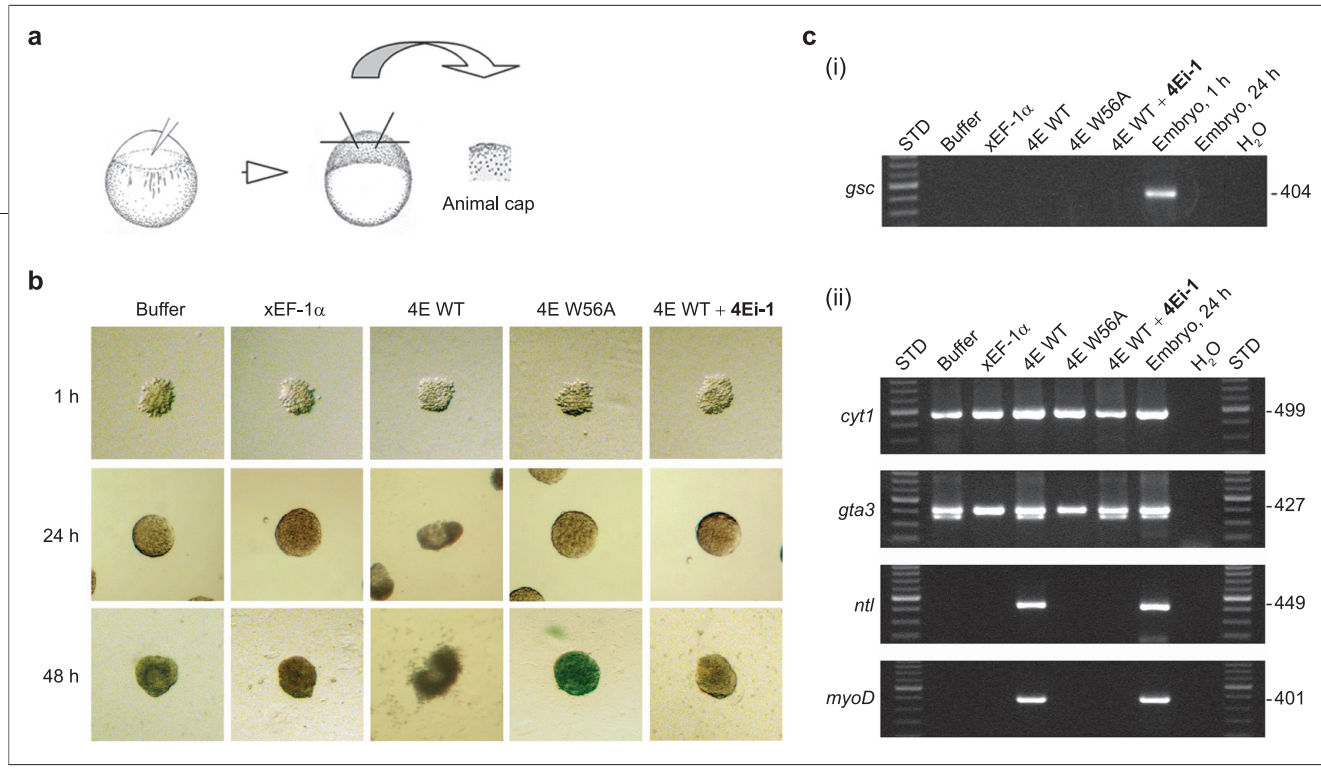

Figure 5. Inhibition of the epithelial-to-mesenchymal transition by 4Ei-1**. a) Experimental setup to analyze the impact of cap-dependent translation alteration in ectoderm blastula explants. Buffer (HBSS); mRNA encoding *Xenopus* elongation factor (xEF-1α, negative control), eIF4E WT or the cap-binding mutant eIF4E W56A, or a mixture of mRNA and** 4Ei-1 **(as indicated) are injected at the one-cell stage. Ectoderm blastula explants are excised prior to germ layer restriction and cultured individually. b) Explant morphology at 1, 24, and 48 h post excision. Within 1 h, explants changed their shape from rectangular to spheroid. Within 24 h, 79% of the explants derived from eIF4E WT-injected embryos (98 of 124) became elongated and developed distinct compartments consisting of two cell types: (i) visually transparent and (ii) opaque. By 48 h, the opaque cells migrated from the explants, assuming positions randomly throughout the culture dish. In contrast, explants derived from embryos injected with buffer or the control xEF-1α mRNA remained spherical for 48 h. Of note, explants derived from embryos injected with either eIF4E W56A or eIF4E WT +** 4Ei-1 **did not differ from control, showing that the ability of eIF4E to bind the mRNA cap is required for development of the motile cell phenotype. c) Stage- and lineage-specific markers. RT-PCR amplified fragments resolved on agarose gel, standards on the left (STD). (i) *goosecoid* (*gsc*) expression. Maternally expressed mesodermal *gsc*, which demarcates future dorsal cells at the lateral portion of the embryo (*59*) was detected only in the intact embryos at the time point corresponding to 1 h post explant excision and in none of the explants, confirming that there were no mesoderm-destined cells present in the explants. (ii). The ectodermal marker *cytokeratin type 1* (*cyt1*) and a ventral cell marker *gta3* (*58, 60*) were observed in all samples, establishing the integrity of the RNA being analyzed and the ectodermal origin of the explants. The notochord mesoderm marker *no tail* (*ntl*) and the paraxial mesoderm marker *myogenic D* (*myoD*) were detected only in explants injected with eIF4E WT mRNA 24 h post excision and in the intact embryos at the expected times.**

Supplementary Figure 4). These data show that **4Ei-1** specifically interdicts EMT, a key step in the genesis of epithelial cell cancers and tissue fibrosis, thus displaying an activity with promise for preventing the evolution of premalignant lesions and cancer in situ to invasive cancer and offering an option for the interdiction of progressive fibrosis.

Mechanism of 4Ei-1 **Inhibition: Activation by HINT.** Despite displaying a low affinity for eIF4E, **4Ei-1** potently inhibited cap-dependent translation *in vitro* and *in vivo* (*vide supra*) and blocked EMT. To elucidate its mechanism of action, we examined the binding of a fluorescent peptide to the eIF4E binding pocket for eIF4G and found that **4Ei-1** did not interfere (data not shown). Thus it is unlikely that **4Ei-1** inhibits cap-dependent translation by blocking eIF4G binding to eIF4E (*17*). Prior studies indicate that 7-BnGMP can inhibit eIF4E binding to the cap analogue, 7-MeGTP (*19*), and we show that 7-BnGMP binds to the cap-binding region in an orientation that compensates for loss of the β phosphate observed for 7-MeGDP. We therefore hypothesized that **4Ei-1** is metabolized in cells releasing the active inhibitor 7-BnGMP. By screening the zebrafish protein database (Entrez. PubMed), we found two sequences, AAH81526.1 and CAI29411.1, that are 73% homologous to the human HINT-1 and HINT-3 enzymes. The presence of HINT activity in the early stages of embryogenesis has been recently demonstrated in bovine embryos as early as the 8-cell stage (*47*). Therefore, we examined zebrafish gastrula lysates for HINT activity and found, based on endogenous phosphoramidase activity, 1.95 ng per 50 μL. This indicates that both rabbit and zebrafish lysates can convert **4Ei-1** to the corresponding monophosphate and suggests that **4Ei-1**, our most potent cap-dependent translation inhibitor, may be a better substrate for HINT hydrolase than either

4Ei-2 or **4Ei-3**. These data are in accord with the idea that **4Ei-1** might be acting as a HINT-bioactive phosphoramidate prodrug of the eIF4E antagonist 7-BnGMP.

Enzymatic Processing of 4Ei-1 **to 7-BnGMP.** To directly determine if **4Ei-1** acted as a HINT-bioactivatable prodrug, we quantified **4Ei-1** and 7-BnGMP as a function of time in both zebrafish embryo and rabbit reticulocyte lysates using liquid chromatography/mass spectrometry (see Methods). Within 1 h after addition of **4Ei-1** (750 μM), complete loss of **4Ei-1** with a concomitant increase in 7-BnGMP was observed (Supplementary Figure 5). As a control, we added **4Ei-1** to heat-inactivated lysates and detected no conversion, instead observing values for **4Ei-1** concentration (1413 ± 16 to 1583 ± 167 ng mL^{-1}) close to the predicted value for the input quantity of **4Ei-1** at 150 μM (1395 ng mL^{-1}). These data indicate that both rabbit and zebrafish cell lysates are fully capable of converting **4Ei-1** to 7-BnGMP, confirming the prodrug mechanism. Our data does not exclude the possibility that other cellular cap-binding proteins such as 4E homologous protein (4EHP) or heterodimeric nuclear cap-binding complex (CBC) might also be targets of **4Ei-1**. However, we view this as unlikely because they have a much lower (1000-fold) affinity for the cap or mononucleotide cap analogues than eIF4E (*48–50*), and to date, neither has ever been implicated in EMT in any biological system.

Conclusions. The EMT is an essential differentiation program in early embryonic development when germ layers and organ topography are established (reviewed in ref 45). The process involves loss of both cell polarity and tight intercellular junctions as ectodermal epithelial cells acquire a nonpolarized, migratory mesenchymal phenotype. However, in some of the most prevalent and morbid human diseases, the EMT is usurped to mediate pathological changes. For example, in cancer the EMT enables epithelial cells to transit the cancer pathway, acquiring the capacity to migrate, invade tissue planes, and metastasize (reviewed in ref 51), and in fibroproliferative diseases of the lung, liver, and kidney, EMT is a source of pathological fibroblasts that deposit connective tissue distorting normal anatomy and thus leading to organ failure (reviewed in ref 52). Despite its importance in human disease, no therapies have been developed to interdict EMT. As a potentially dispensable process in adults that is central to the pathogenesis of cancer and fibrosis, compounds targeting EMT could in principle be robust therapeutic agents without significant toxicity.

METHODS

General Synthetic Procedures and Materials. All reagents were purchased from commercial vendors and used without further purification. Dowex 50WX8-200 cation exchange column was converted to its Na^+ form by treatment with 1 N NaOH, followed by washing with water to bring the pH to neutrality. 1-Ethyl-3-(3-dimethyllaminopropyl)carbodiimide hydrochloride (EDC) was used from a previously unopened bottle. Analytical thin layer chromatorgraphy (TLC) was performed on 0.25 mm precoated Merck silica gel (SiO_2) 60 F_{254}. Column chromatography was performed on Purasil 60A silica gel, 230–400 mesh (Whatman). ^1H and ^{31}P NMR were recorded on a Varian Mercury-300 spectrometer. Chemical shifts are reported in ppm relative to residual deuterium oxide (D_2O) or external indicator 85% H_3PO_4 peaks for ^1H and ^{31}P NMR, respectively. High-resolution mass spectrometry (HRMS) data were obtained on a Biotof II (Bruker) ESI-MS spectrometer. 7-Bn-guanosine monophosphate (7-BnGMP, disodium salt) was synthesized according to established methods (*40*).

Phosphoramidate Synthesis. Compound **4Ei-1** was synthesized as described earlier (*29*), and a slight modification of the same procedure, as outlined below, was used in the preparation of compounds **4Ei-2** and **4Ei-3**. 7-Bn-Guanosine monophosphate disodium salt (0.100 g, 0.200 mmol) and the appropriate amino acid methyl ester hydrochloride salt (D-phenylalanine methyl ester·HCl for **4Ei-2** and D-alanine methyl ester·HCl for **4Ei-3**, 1.01 mmol, 5 equiv) were dissolved in H_2O (5 mL), and the pH of the solution was adjusted to ~7.20 by dropwise addition of dilute aqueous NaOH. To the foregoing was added EDC (0.192 g, 1.01 mmol, 5 equiv) dissolved in 2 mL of 2 mM *N*-methylmorpholine (pH = 7.0), and the resultant solution allowed to stir at RT overnight. Upon complete consumption of the nucleotide starting material (TLC and ^{31}P NMR), the product mixture was concentrated *in vacuo*, and the residue was chromatographed on silica gel, eluting with $CHCl_3$/MeOH/H_2O (5:2:0.25, containing 0.5% NH_4OH). The solid obtained, EDC salt of the phosphoramidate, after evaporation of the solvent was passed through an ion-exchange column (Dowex-50WX8-200, Na^+ form), and the relevant fractions were pooled and lyophilized to give the desired phosphoramidate sodium salts as white amorphous solids in 35–40% yield.

Compound **4Ei-2**: ^1H NMR (D_2O, 300 MHz) δ 7.22–7.26 (m, 5H), 7.07–7.06 (m, 3H), 6.86 (d, 2H), 5.81 (d, 1H), 5.38 (dd, 2H), 4. 54 (m, 1H), 4.23 (t, 1H), 4.12 (m, 1H), 3.81 (dd, 2H), 3.65 (t, 1H), 3.31 (s, 3H), 2.61 (m, 2H) ppm. ^{31}P (D_2O, 121 MHz) δ 7.11 ppm. HRMS (ESI): *m*/*z* calcd for $C_{27}H_{31}N_6NaO_9P^+$ $(M)^+$ 637.1788, found 637.1785.

Compound **4Ei-3**: ^1H NMR (D_2O, 300 MHz) δ 7.25–7.26 (m, 5H), 5.90 (t, 1H), 5.52 (dd, 2H), 4. 53 (m, 1H), (4.19–4.27, 2m, 2H), 3.91 (dd, 2H), 3.52 (t, 1H), 3.38 (s, 3H), 1.07 (d, 3H) ppm. ^{31}P (D_2O, 121 MHz) δ 7.26 ppm. HRMS (ESI): *m*/*z* calcd for $C_{21}H_{27}N_6NaO_9P^+$ $(M)^+$ 561.1469, found 561.1474.

As is the case with most 7-benzylated guanosines, the signal due to the C-8 proton was not observed for either of the two compounds because of its rapid exchange with protons from the NMR solvent.

Fluorescence Titrations and Determination of K_d. The concentration of eIF4E was optimized to 200 nM and was used for all titration experiments, which was duplicated for each compound. Fluorescence spectra were recorded on a Cary Eclipse fluorescence spectrophotometer. Titration experiments were carried out at 22 °C with freshly prepared HEPES buffer (50 mM Hepes, 100 mM KCl, 1 mM DTT, 0.5 mM EDTA) at pH 7.2. Nonlinear fitting was carried out using the statistics software JMP IN 4.0 (SAS Institute) in which the following equation was applied:

$$F = \frac{(P_t + L_t + K_d - \sqrt{(P_t + L_t + K_d)^2 - 4P_tL_t})(F - F_b)}{2P_t}$$

where F = fluorescence intensity of protein without ligand binding; F_b = fluorescence intensity of protein with ligand binding; P_t = total concentration of the protein; L_t = total concentration of the ligand; and K_d = dissociation constant (*40*).

Each titration was duplicated, and two parallel correction experiments were carried out corresponding to the increase in fluorescence intensity by the intrinsic fluorescence of the cap analogues and decrease in fluorescence due to eIF4E degradation and dilution effect. A series of ligand stocks at 20 μM, 50 μM, 100 μM, 250 μM, 500 μM, 1 mM, 2 mM, and 5 mM were prepared in order to obtain smooth titration curves by minimizing titration errors.

Cell-Free Translation Assay. To directly assess the level of translation, we employed the dual-luciferase bicistronic reporter construct pcDNA3-rLuc-POLIRES-fLuc (*42*), which is designed so that the translation of *Renilla reniformis* luciferase (rLUC) is strictly cap-dependent, whereas the translation of firefly luciferase (fLUC) proceeds *via* an IRES in a cap-independent manner. The template encodes two forms of luciferase, each producing a product emitting light at a unique wavelength. The plasmid was linearized with *Xma*I, purified from an agarose gel, and 5′-capped bicistronic luciferase reporter mRNA was generated by *in vitro* transcription (mMESSAGE mMACHINE kit, Ambion) using T7 polymerase, according to the manufacturer's instructions. Reporter mRNA (0.02 μg) was added to the reaction mixture (17 μL Retic lysate, 1 μL 1.25 mM L-methionine, 1.25 μL translation buffer per reaction), as recommended (Retic Lysate IVT, Ambion). *Renilla* luciferase translation was carried out at high ionic strength conditions (high salt mix, 150 mM potassium chloride), whereas firefly luciferase was at low ionic strength conditions (low salt mix, 25 mM potassium chloride). Test compounds or nuclease-free water (control) were introduced into the reaction mixture. *In vitro* translation was carried out at 30 °C for 1 h. The reaction was stopped by chilling (5 min on ice), and samples were diluted with 100 μL of nuclease-free water. *Renilla* and firefly luciferase activity/abundance was quantified by luminometry using the Dual-Luciferase Reporter Assay System (Promega) exactly as described in the technical manual, in a Lumat LB 9507 Luminometer (EG&G Berthold). Luminescence was measured in relative light units. Reporter translation in the samples was compared to the control, set at 100. Assays were performed in triplicate; the mean ± SEM values were determined for each compound concentration. To calculate IC_{50}, the compounds were tested at concentrations ranging from 2 to 2000 μM. Data in triplicate corresponding to each concentration were plotted, and the IC_{50} values were determined directly from the plot.

Fish and Embryos. Adult zebrafish (*D. rerio*) maintenance, husbandry, and embryo collection were performed at the Zebrafish Research Core Facility (Arnold and Mabel Beckman Center for Transposon Research) using standard procedures (*53*) with approval from the Institutional Animal Care and Use Committee at the University of Minnesota. Freshly fertilized eggs were obtained through natural spawning. Eggs were staged for microinjections according to earlier precedents (*54*). Embryos were kept at 28.5 °C (standard temperature) and staged according to Kimmel *et al.* (*55*).

Microinjections. Microinjections, embryo observation, and image acquisition were performed on the stage of a Stemi-2000 stereomicroscope (Carl Zeiss MicroImaging, Inc.) equipped with a PowerShot A630 digital camera (Canon) and PLI 100 Pico-injector (Warner Instruments, LLC) at RT. Eggs in chorions were lined up and restrained in the agar grooves (*53*) with their animal poles upward. Reporter mRNA solution (3 nL) was injected into the egg cytoplasm in the geometric center of the yolk depression (15 min post fertilization) through a micropipet with a splinted sharp tip 2–3 μm in diameter. Test compounds were diluted to the final concentration with HBSS (Gibco) containing 0.03% phenol red (Sigma). Compound-containing medium (5 nL) was microinjected into the cytoplasm during furrow progression at the 2-cell stage in the second round of microinjections, performed through the opening in chorions made by the first injection. Sham-treated eggs (negative control) were injected with 5 nL of the carrier (HBSS). Eggs were kept at 28.5 °C.

Zebrafish Translation Assay. Reporter mRNA was diluted with HBSS (Gibco) containing 0.03% phenol red (Sigma) to a concentration of 200 ng μL^{-1}. Aliquots were stored at −80 °C until needed. Luciferase reporters were expressed ectopically after RLUC-POLIRES-FLUC mRNA injection into the single-cell fertilized eggs. We employed reporter in the form of mRNA, because transcripts are evenly distributed among dividing zebrafish embryonic cells after injection into fertilized eggs and are translated into protein within the first day of development (*56*). Eggs were first injected with the bicistronic luciferase mRNA (0.5 ng) and then with test compound in doses ranging from 5 to 25 pmols, with 7-MeGTP (reference compound) or with the carrier (HBSS). To standardize the level of luciferase expression across the injected eggs, we used a stringent microinjection protocol (one micro-needle per series, with no recalibration or readjustment of injection parameters). To ensure stable results, we normalized luciferase readouts to the number of eggs and utilized greater than 20 embryos ($n \geq 20$) per sample. In each series of experiments, eggs were injected continuously (groove after groove), and for drug administration in groups comprising equal numbers of eggs from all grooves. The second injection was performed through the opening in the egg's chorion made by the first injection. In assay validation using CHD (single dose, 0.1 pmol), the estimated error range for precision and accuracy of the zebrafish translation assay was determined to be within 15%. Normally developing embryos were harvested at the early gastrula stage (28.5 °C, 4.5 h after injection). Firefly and *Renilla* luciferase activities were analyzed using the Luciferase Reporter Assay system (Promega). Luciferase assays were performed in triplicate according to the manufacturer's instruction in a Lumat LB 9507 (EG&G Berthold).

Ectoderm Explant Extraction and Cultivation. Ectoderm explants ("animal caps") were surgically removed from the apical region of late blastulae (stages Sphere-Dome, 4–4.3 hpf) at 28.5 °C in sterile Modified Barth's saline (MBS) using established procedures (*57*) with the following modifications: square blocks of superficial apical blastoderm comprised approximately 70 cells in 3–4 tiers with a portion of the outer enveloping layer, and explants were cultivated separately in sterile MBS without antibiotics on agar with a 3% methyl cellulose cushion at 28.5 °C for up to 48 h. Under these carefully controlled conditions, ectoderm blastula explants retain a spherical shape and contain dividing cells destined only to an ectodermal fate (*57, 58*). In unfavorable conditions, explants decompose and largely dissipate within 24 h in culture. Explants from injected em-

TABLE 3. Oligonucleotide primers used for RT-PCR

Marker	Forward primer (5′–3′)	Reverse primer (3′–5′)	Size
cyt1	GGGGCGCAGGATTTGGTG	GTTCTTCTTGGTGCTCCTCCTCGA	499
gta3	CCTGGGCCTCTGTCCGTCTATCCT	CTCTTACACATTTGACGCCCCGGT	427
gsc	ACGGCAGCTGGCGATTTTA	CTTTATGGGACTGCAGCCGTG	404
ntl	GCCCGAGCTGCGTCTACATCC	GGAGTCAAGTTACCCCGGGGA	449
myoD	CTTAAACCCGACGAGCATCAC	TACTACCTAAAATACCCGGG	401

bryos or intact embryos (as a positive control) were harvested at two time points corresponding to 1 and 24 h post excision and analyzed by RT-PCR for lineage and stage specific transcripts.

Immunoblot Analysis. Whole-embryo lysates were prepared from normally developing embryos (20 per sample). Eggs were rinsed with HBSS, dispersed in lysis buffer (50 mM Tris-HCl (pH 7.5), 250 mM NaCl, 50 mM NaF, 5 mM EDTA, 0.2% NP-40) with protease inhibitor cocktail (Complete MINI, Roche) on ice, kept on a shaker for 20min at 4 °C, and centrifuged at 16,000*g* for 15 min with the supernatant retained. Protein concentration in the supernatant was measured using the BCA protein assay kit (Pierce). Twenty micrograms of protein was subjected to 8% SDS-PAGE under reducing conditions and transferred to nitrocellulose. Immuno-detection of proteins was carried out using primary antibodies (Rat anti-HA, 1:2000) followed by horseradish peroxidase-conjugated secondary antibodies (antirat IgG, 1:500) and incubation with chemiluminescence substrate (Pierce).

RT-PCR. RNA was extracted using TRI reagent (Sigma). The RNA samples were treated with DNAase using Turbo DNA-free kit (Ambion) according to the manufacturer's directions and converted to cDNA using the TaqMan reverse transriptase kit (Roche). Real-time PCR was performed using the Roche Light-Cycler with SYBR Green dye according to the manufacturer's protocol (Roche). Amplified fragments were resolved on 1% agarose gels and sized according to standards. The sequences of the primers and the size of amplificate (bp) are provided in Table 3 for each gene analyzed.

Amplified fragments were resolved on 1% acrylamide gels and visualized by BrdU staining. Gel images were acquired with a UVP BioDoc-it™ System.

HINT Activity in the Rabbit Reticulocyte and Zebrafish Gastrula Lysates. Activity of HINT was quantified by individually titrating 20 μL of rabbit reticulocyte lysate and 50 μL of zebrafish gastrula lysate (both in 600 μL HEPES) against 30 μL of the fluorogenic substrate, AMP-tryptamine phosphoramidate (*34*). The observed increase in fluorescence intensity was plotted against time, and the slope of the rectilinear plots was substituted in the following equation to obtain the value of the enzyme concentrations:

$$v = \frac{\text{slope}}{F_{pro} - F_{sub}} = k_{cat}E_t$$

where v = velocity; F_{pro} = fluorescence due to product (tryptamine); F_{sub} = fluorescence due to substrate (AMP-tryptamine phosphoramidate); and E_t = total enzyme concentration. k_{cat} for AMP-tryptamine phosphoramidate = 2.1 ± 0.1 s^{-1}. The rabbit reticulocyte and zebrafish embryo lysates contain 23 and 1.95 ng of the enzyme, respectively.

Liquid Chromatography/Mass Spectrometry (LC-MS/MS) of 4Ei-1 Metabolism. Rabbit reticulocyte lysate (Ambion) and zebrafish embryo lysates were used in studying **4Ei-1** conversion. In the zebrafish lysate preparation, 300 early pre-gastrula eggs were collected, washed with "embryo medium", dried, and mechanically homogenized. The crude homogenate was kept rotating for 30 min at 4 °C, centrifuged (15 min, 12,000 rpm at 4 °C) with supernatant fluid retained, and designated embryo lysate. All standard solutions and samples were kept on ice before analysis by LC-MS/MS. *N*,*N*-Dimethylhexylamine (DMHA), tetrabutyl ammonium acetate (TBAA), and ammonium acetate were purchased from Sigma. Solvents used for LC analysis were HPLC grade. All solutions for instrument analyses were filtered through a 0.22 μm membrane filter and degassed prior to use. Microcon microcentrifuge filter device YM-10 (molecular weight cutoff 10,000) was purchased from Millipore. Chromatographic separation was achieved using a narrow bore Eclipse XDB-C18 column (2.1 mm × 50 mm, 1.8 μm, Agilent Technologies) eluted at a flow rate of 0.125 mL min^{-1}. An injection volume of 10 μL was used for standards and lysates. The mobile phase was composed of 50% solvent A (10 mM ammonium acetate, pH 6.65) and 50% solvent B (methanol). The running time for each sample was 5 min. Sample temperature was maintained at 4 °C with a thermostat-controlled sample compartment. A TSQ quantum classic LC-ESI-MS/MS system (Agilent 1200 LC) was employed for all analyses. The mass spectrometer was operated in negative ion mode with nitrogen as a nebulizing and drying gas. 7-BnGMP and **4Ei-1** were directed to the detector for infusion. ESI source parameters and MS/MS parameters were optimized for maximum sensitivity. Negative ion ESI and selective multiple reaction monitoring (MRM) mode was used in all analyses. The $[M - H]^-$ ion of 7-BnGMP (*m*/*z* 452.10) was isolated and subjected to collision-induced dissociation (CID) to give the product ion (*m*/*z* 79.19, collision energy 52 V) for quantification. **4Ei-1** was analyzed analogously to give a parent ion (*m*/*z* 594.00) and product ion (*m*/*z* 148.84, collision energy 52 V). The standard curves were obtained in respective matrix with a known concentration of 7-BnGMP and **4Ei-1** ranging from 10 to 10,000 ng mL^{-1}. Quantification of target compounds was carried out with XCalibur software (Thermo Scientific). Rabbit and zebrafish lysates were diluted 64-fold with 10 mM ammonium acetate (pH 6.65) and methanol in a ratio of 1:1, followed by heating at 50 °C for 30 min. Precipitates were filtered using microcon YM-10 (Millipore). The filtrate served as matrix for preparing standard solutions. Ten microliters of a known concentration (100, 500, 1000, 5000, 10000, 50000, 100000 ng mL^{-1}) of both targets dissolved in methanol was added to a HPLC sample vial. Methanol was removed in a SC210A SpeedVac concentrator (Thermo Scientific). Lysate matrix (100 μL) was added to each concentrated vial to make the corresponding standard solutions (10, 50, 100, 500, 1000, 5000, 10000 ng mL^{-1}). For sample preparation, **4Ei-1** (5 μL) at 150 μM (final concentration)

was incubated with lysates (17 μL) at 30 °C for 1 h, followed by similar treatment (with or without heating at 50 °C for 30 min) as the standards. Controls were prepared in the same way except that dH_2O (Sigma) substituted for **4Ei-1**.

Acknowledgment: The authors thank C. Sagerström for advice regarding the explant experiments. This work was supported by the National Institute of Health grants 1R01 HL076779 and 1R21RR024398 (P.B.B and A.O.B.), 5U01-CA091220 (V.A.P.), and University of Minnesota AHC Faculty Development Grant (C.R.W.).

Supporting Information Available: This material is available free of charge *via* the Internet at http://pubs.acs.org.

REFERENCES

1. Gingras, A. C., Raught, B., and Sonenberg, N. (1999) eIF4 initiation factors: effectors of mRNA recruitment to ribosomes and regulators of translation, *Annu. Rev. Biochem. 68*, 913–963.
2. Gallie, D. R. (2002) Protein−protein interactions required during translation, *Plant Mol. Biol. 50*, 949–970.
3. Pestova, T. V., and Hellen, C. U. (2001) Functions of eukaryotic factors in initiation of translation, *Cold Spring Harbor Symp. Quant. Biol. 66*, 389–396.
4. Browing, K. S. (1996) The plant translational apparatus, *Plant Mol. Biol. 32*, 107–144.
5. Gallie, D. R. (1998) A tale of two termini: a functional interaction between the termini of an mRNA is a prerequisite for efficient translation initiation, *Gene 216*, 1–11.
6. Gingras, A. C., Raught, B., and Sonenberg, N. (2004) mTOR signaling to translation, *Curr. Top. Microbiol. Immunol. 279*, 169–197.
7. Polunovsky, V. A., and Bitterman, P. B. (2006) The cap-dependent translation apparatus integrates and amplifies cancer pathways, *RNA Biol. 3*, 10–17.
8. Raught, B., and Gingras, A. C. (1999) eIF4E activity is regulated at multiple levels, *Int. J. Biochem. Cell Biol. 31*, 43–57.
9. Sonenberg, N., and Gingras, A. C. (1998) The mRNA 5′ cap-binding protein eIF4E and control of cell growth, *Curr. Opin. Cell Biol. 10*, 268–275.
10. Richter, J. D., and Theurkauf, W. E. (2001) Development. The message is in the translation, *Science 293*, 60–62.
11. Vasudevan, S., Seli, E., and Steitz, J. A. (2006) Metazoan oocyte and early embryo development program: a progression through translation regulatory cascades, *Genes Dev. 20*, 138–146.
12. Avdulov, S., Li, S., Michalek, V., Burrichter, D., Peterson, M., Perlman, D. M., Manivel, J. C., Sonenberg, N., Yee, D., and Bitterman, P. B., *et al.* (2004) Activation of translation complex eIF4F is essential for the genesis and maintenance of the malignant phenotype in human mammary epithelial cells, *Cancer Cell 5*, 553–563.
13. Larsson, O., Li, S., Issaenko, O. A., Avdulov, S., Peterson, M., Smith, K., Bitterman, P. B., and Polunovsky, V. A. (2007) Eukaryotic translation initiation factor 4E induced progression of primary human mammary epithelial cells along the cancer pathway is associated with targeted translational deregulation of oncogenic drivers and inhibitors, *Cancer Res. 67*, 6814–6824.
14. Ruggero, D., Montanaro, L., Ma, L., Xu, W., Londei, P., Cordon-Cardo, C., and Pandolfi, P. P. (2004) The translation factor eIF-4E promotes tumor formation and cooperates with c-Myc in lymphomagenesis, *Nat. Med. 10*, 484–486.
15. Zimmer, S. G., DeBenedetti, A., and Graff, J. R. (2000) Translational control of malignancy: the mRNA cap-binding protein, eIF-4E, as a central regulator of tumor formation, growth, invasion and metastasis, *Anticancer Res. 20*, 1343–1351.
16. Graff, J. R., Konicek, B. W., Carter, J. H., and Marcusson, E. G. (2008) Targeting the eukaryotic translation initiation factor 4E for cancer therapy, *Cancer Res. 68*, 631–634.
17. Moerke, N. J., Aktas, H., Chen, H., Cantel, S., Reibarkh, M. Y., Fahmy, A., Gross, J. D., Degterev, A., Yuan, J., and Chorev, M., *et al.* (2007) Small-molecule inhibition of the interaction between the translation initiation factors eIF4E and eIF4G, *Cell 128*, 257–267.
18. Graff, J. R., Konicek, B. W., Vincent, T. M., Lynch, R. L., Monteith, D., Weir, S. N., Schwier, P., Capen, A., Goode, R. L., and Dowless, M. S., *et al.* (2007) Therapeutic suppression of translation initiation factor eIF4E expression reduces tumor growth without toxicity, *J. Clin. Invest. 117*, 2638–2648.
19. Ghosh, P., Park, C., Peterson, M. S., Bitterman, P. B., Polunovsky, V. A., and Wagner, C. R. (2005) Synthesis and evaluation of potential inhibitors of eIF4E cap binding to 7-methyl GTP, *Bioorg. Med. Chem. Lett. 15*, 2177–2180.
20. Grudzien, E., Stepinski, J., Jankowska-Anyszka, M., Stolarski, R., Darzynkiewicz, E., and Rhoads, R. E. (2004) Novel cap analogs for *in vitro* synthesis of mRNAs with high translational efficiency, *RNA 10*, 1479–1487.
21. Wagner, C. R., Iyer, V. V., and McIntee, E. J. (2000) Pronucleotides: toward the *in vivo* delivery of antiviral and anticancer nucleotides, *Med. Res. Rev. 20*, 417–451.
22. Meier, C. (1998) Pronucleotides: Recent advances in the design of efficient tools for the delivery of biologically active nucleoside monophosphates, *Synlett* 233–242.
23. Wagner, C. R., Chang, S. L., Griesgraber, G. W., Song, H., McIntee, E. J., and Zimmerman, C. L. (1999) Antiviral nucleoside drug delivery via amino acid phosphoramidates, *Nucleosides Nucleotides 18*, 913–919.
24. Chang, S., Griesgraber, G. W., Southern, P. J., and Wagner, C. R. (2001) Amino acid phosphoramidate monoesters of 3′-azido-3′-deoxythymidine: relationship between antiviral potency and intracellular metabolism, *J. Med. Chem. 44*, 223–231.
25. McGuigan, C., Harris, S. A., Daluge, S. M., Gudmundsson, K. S., McLean, E. W., Burnette, T. C., Marr, H., Hazen, R., Condreay, L. D., and Johnson, L., *et al.* (2005) Application of phosphoramidate pronucleotide technology to abacavir leads to a significant enhancement of antiviral potency, *J. Med. Chem. 48*, 3504–3515.
26. Song, H., Griesgraber, G. W., Wagner, C. R., and Zimmerman, C. L. (2002) Pharmacokinetics of amino acid phosphoramidate monoesters of zidovudine in rats, *Antimicrob. Agents Chemother. 46*, 1357–1363.
27. Song, H., Johns, R., Griesgraber, G. W., Wagner, C. R., and Zimmerman, C. L. (2003) Disposition and oral bioavailability in rats of an antiviral and antitumor amino acid phosphoramidate prodrug of AZT-monophosphate, *Pharm. Res. 20*, 448–451.
28. Chou, T. F., Bieganowski, P., Shilinski, K., Cheng, J., Brenner, C., and Wagner, C. R. (2005) 31P NMR and genetic analysis establish hinT as the only *Escherchia coli* purine nucleoside phosphoramidase and as essential for growth under high salt conditions, *J. Biol. Chem. 280*, 15356–15361.
29. Chou, T. F., Baraniak, J., Kaczmarek, R., Zhou, X., Cheng, J., Ghosh, B., and Wagner, C. R. (2007) Phosphoramidate pronucleotides: a comparison of the phosphoramidase substrate specificity of human and *Escherichia coli* histidine triad nucleotide binding proteins, *Mol. Pharm. 4*, 208–217.
30. Kim, J., Chou, T. F., Griesgraber, G. W., and Wagner, C. R. (2004) Direct measurement of nucleoside monophosphate delivery from a phosphoramidate pronucleotide by stable isotope labeling and LC-ESI(−)-MS/MS, *Mol. Pharm. 1*, 102–111.
31. Yuan, B. Z., Jefferson, A. M., Popescu, N. C., and Reynolds, S. H. (2004) Aberrant gene expression in human non small cell lung carcinoma cells exposed to demethylating agent 5-aza-2′-deoxycytidine, *Neoplasia 6*, 412–419.
32. Sahlgren, C., Gustafsson, M. V., Jin, S., Poellinger, L., and Lendahl, U. (2008) Notch signaling mediates hypoxia-induced tumor cell migration and invasion, *Proc. Natl. Acad. Sci. U.S.A. 105*, 6392–6397.

33. Korpal, M., Lee, E. S., Hu, G., and Kang, Y. (2008) The miR-200 family inhibits epithelial-mesenchymal transition and cancer cell migration by direct targeting of E-cadherin transcriptional repressors ZEB1 and ZEB2, *J. Biol. Chem. 283*, 14910–14914.
34. Gavert, N., and Ben-Ze'ev, A. (2008) Epithelial-mesenchymal transition and the invasive potential of tumors, *Trends Mol. Med. 14*, 199–209.
35. Park, S. M., Gaur, A. B., Lengyel, E., and Peter, M. E. (2008) The miR-200 family determines the epithelial phenotype of cancer cells by targeting the E-cadherin repressors ZEB1 and ZEB2, *Genes Dev. 22*, 894–907.
36. Gregory, P. A., Bert, A. G., Paterson, E. L., Barry, S. C., Tsykin, A., Farshid, G., Vadas, M. A., Khew-Goodall, Y., and Goodall, G. J. (2008) The miR-200 family and miR-205 regulate epithelial to mesenchymal transition by targeting ZEB1 and SIP1, *Nat. Cell Biol. 10*, 593–601.
37. Mani, S. A., Guo, W., Liao, M. J., Eaton, E. N., Ayyanan, A., Zhou, A. Y., Brooks, M., Reinhard, F., Zhang, C. C., and Shipitsin, M., *et al.* (2008) The epithelial-mesenchymal transition generates cells with properties of stem cells, *Cell 133*, 704–715.
38. Burk, U., Schubert, J., Wellner, U., Schmalhofer, O., Vincan, E., Spaderna, S., and Brabletz, T. (2008) A reciprocal repression between ZEB1 and members of the miR-200 family promotes EMT and invasion in cancer cells, *EMBO Rep. 9*, 582–589.
39. Cai, A., Jankowska-Anyszka, M., Centers, A., Chlebicka, L., Stepinski, J., Stolarski, R., Darzynkiewicz, E., and Rhoads, R. E. (1999) Quantitative assessment of mRNA cap analogues as inhibitors of *in vitro* translation, *Biochemistry 38*, 8538–8547.
40. Niedzwiecka, A., Marcotrigiano, J., Stepinski, J., Jankowska-Anyszka, M., Wyslouch-Cieszynska, A., Dadlez, M., Gingras, A. C., Mak, P., Darzynkiewicz, E., and Sonenberg, N., *et al.* (2002) Biophysical studies of eIF4E cap-binding protein: recognition of mRNA 5′ cap structure and synthetic fragments of eIF4G and 4E-BP1 proteins, *J. Mol. Biol. 319*, 615–635.
41. Brown, C. J., McNae, I., Fischer, P. M., and Walkinshaw, M. D. (2007) Crystallographic and mass spectrometric characterisation of eIF4E with N7-alkylated cap derivatives, *J. Mol. Biol. 372*, 7–15.
42. Poulin, F., Gingras, A. C., Olsen, H., Chevalier, S., and Sonenberg, N. (1998) 4E-BP3, a new member of the eukaryotic initiation factor 4E-binding protein family, *J. Biol. Chem. 273*, 14002–14007.
43. Stern, H. M., and Zon, L. I. (2003) Cancer genetics and drug discovery in the zebrafish, *Nat. Rev. Cancer 3*, 533–539.
44. Zon, L. I., and Peterson, R. T. (2005) *In vivo* drug discovery in the zebrafish, *Nat. Rev. Drug Discovery 4*, 35–44.
45. Thiery, J. P., and Sleeman, J. P. (2006) Complex networks orchestrate epithelial-mesenchymal transitions, *Nat. Rev. Mol. Cell. Biol. 7*, 131–142.
46. Klein, P. S., and Melton, D. A. (1994) Induction of mesoderm in *Xenopus laevis* embryos by translation initiation factor 4E, *Science 265*, 803–806.
47. Goossens, K., Van Soom, A., Van Poucke, M., Vandaele, L., Vandesompele, J., Van Zeveren, A., and Peelman, L. J. (2007) Identification and expression analysis of genes associated with bovine blastocyst formation, *BMC Dev. Biol. 7*, 64.
48. Zuberek, J., Kubacka, D., Jablonowska, A., Jemielity, J., Stepinski, J., Sonenberg, N., and Darzynkiewicz, E. (2007) Weak binding affinity of human 4EHP for mRNA cap analogs, *RNA 13*, 691–697.
49. Izaurralde, E., Stepinski, J., Darzynkiewicz, E., and Mattaj, I. W. (1992) A cap binding protein that may mediate nuclear export of RNA polymerase II-transcribed RNAs, *J. Cell Biol. 118*, 1287–1295.
50. Worch, R., Niedzwiecka, A., Stepinski, J., Mazza, C., Jankowska-Anyszka, M., Darzynkiewicz, E., Cusack, S., and Stolarski, R. (2005) Specificity of recognition of mRNA 5′ cap by human nuclear cap-binding complex, *RNA 11*, 1355–1363.
51. Peinado, H., Olmeda, D., and Cano, A. (2007) Snail, Zeb and bHLH factors in tumour progression: an alliance against the epithelial phenotype? *Nat. Rev. Cancer 7*, 415–428.
52. Radisky, D. C., Kenny, P. A., and Bissell, M. J. (2007) Fibrosis and cancer: do myofibroblasts come also from epithelial cells via EMT? *J. Cell. Biochem. 101*, 830–839.
53. Westerfield, M. (1995) *The Zebrafish Book*, 3rd ed., Institute of Neuroscience, Eugene, OR.
54. Benyumov, A. O., Dubrovskaya, T. A., Barmintsev, V. A., and Shan, L. (1995) Duration of the first mitotic cycles and staging of embryogenesis of *Danio rerio*, *Russ. J. Dev. Biol. 26*, 132–138.
55. Kimmel, C. B., Ballard, W. W., Kimmel, S. R., Ullmann, B., and Schilling, T. F. (1995) Stages of embryonic development of the zebrafish, *Dev. Dyn. 203*, 253–310.
56. Wang, X., Wan, H., Korzh, V., and Gong, Z. (2000) Use of an IRES bicistronic construct to trace expression of exogenously introduced mRNA in zebrafish embryos, *Biotechniques 29*, 814–816.
57. Grinblat, Y., Lane, M. E., Sagerstrom, C., and Sive, H. (1999) Analysis of zebrafish development using explant culture assays, *Methods Cell Biol. 59*, 127–156.
58. Sagerstrom, C. G., Grinbalt, Y., and Sive, H. (1996) Anteroposterior patterning in the zebrafish, *Danio rerio*: an explant assay reveals inductive and suppressive cell interactions, *Development 122*, 1873–1883.
59. Gritsman, K., Zhang, J., Cheng, S., Heckscher, E., Talbot, W. S., and Schier, A. F. (1999) The EGF-CFC protein one-eyed pinhead is essential for nodal signaling, *Cell 97*, 121–132.
60. Sagerstrom, C. G., Gammill, L. S., Veale, R., and Sive, H. (2005) Specification of the enveloping layer and lack of autoneuralization in zebrafish embryonic explants, *Dev. Dyn. 232*, 85–97.
61. Marcotrigiano, J., Gingras, A. C., Sonenberg, N., and Burley, S. K. (1997) Cocrystal structure of the messenger RNA 5′ cap-binding protein (eIF4E) bound to 7-methyl-GDP, *Cell 89*, 951–961.
62. Joshi, B., Lee, K., Maeder, D. L., and Jagus, R. (2005) Phylogenetic analysis of eIF4E-family members, *BMC Evol. Biol. 5*, 48.